Electronic Supplementary Material (ESI) for ChemComm.

Supporting information

Asymmetric Chlorination of A_2-A_1-D-A_1-A_2 type Non-fullerene Acceptors for High-Voltage Organic Photovoltaics

*Peiqing Cong[1,2‡], Xianda Li[1,3‡], Ailing Tang[*2], Jiang Wu[1,3], Jianhua Chen[4], Lie Chen[5], Erjun Zhou[1,2*]*

[1] CAS Key Laboratory of Nanosystem and Hierarchical Fabrication, CAS Center for Excellence in Nanoscience, National Center for Nanoscience and Technology, Beijing 100190, China.

[2] Center of Materials Science and Optoelectronics Engineering, University of Chinese Academy of Sciences, Beijing 100049, China.

[3] Henan Institute of Advanced Technology, Zhengzhou University, Zhengzhou 450003, China.

[4] Department of Chemical Science and Technology, Yunnan University, Kunming 650091, China.

[5] College of Chemistry, Nanchang University, 999 Xuefu Avenue, Nanchang, 330031 China

[‡] *These two authors contributed equally to this work*

E-mail: tangal@nanoctr.cn; zhouej@nanoctr.cn

1. Experimental Section

Materials and Synthesis procedure.

All the reagents were purchased from commercial sources and used without further purification. **M2** and **M4** are previously reported by our group[1, 2].

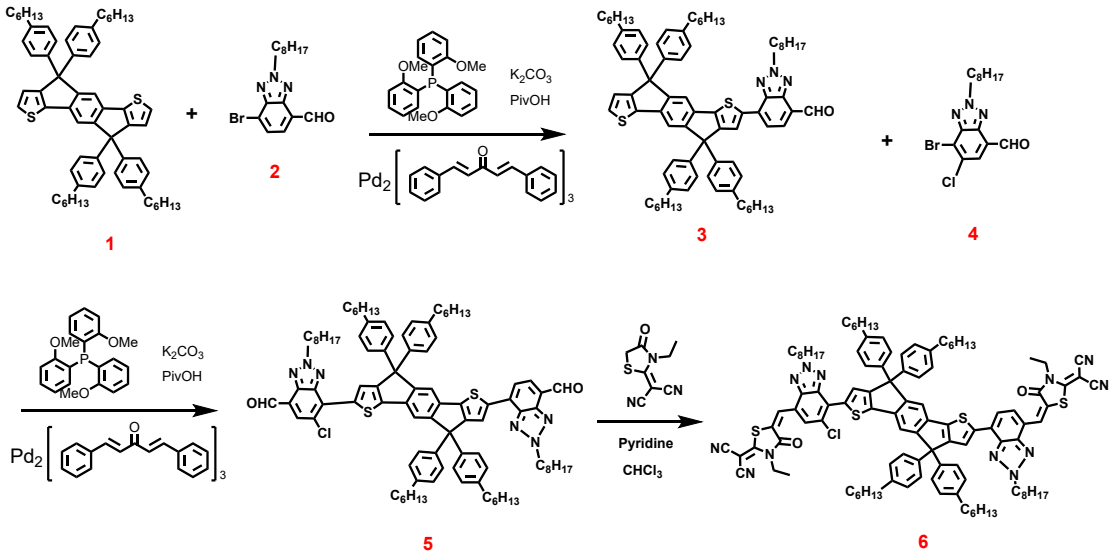

Scheme S1: The synthesis route of the HCl-BTA3.

Synthesis of compound 3:

Compound 1 (907 mg, 1.0 mol), **compound 2** (372 mg, 1.1 mmol), K_2CO_3 (691 mg, 5.0 mmol), PivOH (51 mg, 0.5 mmol), Pb_2bda_3 (45.8 mg, 0.05 mmol), $(_O\text{-MeOPh})_3P$ (35.2 mg, 0.1 mmol) and anhydrous o-xylene (5 mL) were successively added into the reaction flask. After exhausting the nitrogen several times to fully remove the oxygen, the mixture was heated and stirred at 100°C for 24 h. The reaction system was cooled and quenched with water, filtered, then washed thoroughly with water. Then the solution was extracted with ethyl acetate, and dried over anhydrous sodium sulfate.

After the removal of the solvent, the residue was purified by silica gel chromatography to obtain a red solid (304 mg, 25%).

^{1}H NMR (400 MHz, $CDCl_3$) δ 10.37 (s, 1H), 8.13 (s, 1H), 7.91 (d, *J* = 7.7 Hz, 1H), 7.72 (d, *J* = 7.6 Hz, 1H), 7.53 (s, 1H), 7.45 (s, 1H), 7.27 (d, *J* = 4.9 Hz, 1H), 7.24 (d, *J* = 8.3 Hz, 4H), 7.17 (d, *J* = 8.3 Hz, 4H), 7.08 (t, *J* = 7.6 Hz, 8H), 7.01 (d, *J* = 4.9 Hz, 1H), 4.84 (t, *J* = 7.4 Hz, 2H), 2.64 – 2.48 (m, 8H), 2.28 – 2.11 (m, 2H), 1.59 (dd, *J* = 14.9, 7.4 Hz, 8H), 1.29 (ddd, *J* = 12.0, 10.9, 7.7 Hz, 34H), 0.89 – 0.84 (m, 15H).

Synthesis of compound 5:

Compound 3 (250 mg, 214.64 μmol), **compound 4** (88 mg, 236.1 μmol), K_2CO_3 (148.32 mg 1.07 mmol), PivOH (13 mg, 118 μmol), Pb_2bda_3 (10 mg, 11.8μmol), $(_O\text{-MeOPh})_3P$ (7.4 mg, 23.6 μmol) and anhydrous o-xylene (1.5 mL) were successively added into the reaction flask. After exhausting the nitrogen several times to fully remove the oxygen, the mixture was heated and stirred at 100°C for 24 h. The reaction system was cooled and quenched with water, filtered, then washed thoroughly with water. Then the solution was extracted with ethyl acetate and dried over anhydrous sodium sulfate. After the removal of the solvent, the residue was purified by silica gel chromatography to obtain a red solid (250 mg, 80%).

^{1}H NMR (400 MHz, $CDCl_3$) δ: 10.67 (s, 1H), 10.38 (s, 1H), 8.14 (s, 1H), 8.10 (s, 1H), 7.92 (s, 1H), 7.75 (s, 1H), 7.63 (s, 1H), 7.56 (d, 2H), 7.27-7.24 (m, 8H), 7.11-7.12 (d, 8H), 4.81-4.87 (dd, 4H), 2.56-2.60 (m, 8H), 2.15-2.60 (m, 4H), 1.58-1.63 (m, 10H), 1.26-1.32 (m, 42H), 0.84-0.87 (q, 18H).

Synthesis of compound 6 (HCl-BTA3):

Compound 5（120 mg, 82.39 μmol）and 2-(3-ethyl-4-oxathiazolidine-2-methylene) malononitrile (35 mg, 181.25μmol), chloroform (10 ml), pyridine (1ml) were added sequentially into the two-neck round-bottomed flasks. The above reaction was going on at 30℃ for 4 h. After the reaction is stopped, the solution was added dropwise to methanol to precipitate and filtered. Then, the solid was purified by silica gel chromatography to obtain a blue-black solid (85 mg, 57%).

^{1}H NMR (400 MHz, CD2Cl2) δ 8.53 (s, 1H), 8.35 (s, 1H), 8.22 (s, 1H), 8.18 (s, 1H), 7.78 (d, J = 8.2 Hz, 2H), 7.66 – 7.57 (m, 3H), 7.31 (dd, J = 8.2, 3.0 Hz, 8H), 7.17 (d, J = 8.2 Hz, 8H), 4.86 (td, J = 7.0, 4.0 Hz, 4H), 4.40 – 4.25 (m, 4H), 2.69 – 2.55 (m, 8H), 2.32 – 2.18 (m, 4H), 1.63 (dt, J = 15.2, 7.5 Hz, 10H), 1.45 – 1.30 (m, 48H), 0.90 (q, J = 6.8 Hz, 18H).

^{13}C NMR (101 MHz, CDCl3) δ 167.22 (s), 167.16 – 166.58 (m), 157.56 (d, J = 11.9 Hz), 154.23 (d, J = 7.9 Hz), 145.94 (s), 144.73 (s), 142.91 (s), 142.40 (s), 141.90 (t, J = 7.2 Hz), 141.60 – 141.09 (m), 140.16 (s), 139.85 (s), 137.15 (s), 135.95 (s), 135.38 (s), 132.31 (s), 131.40 (s), 129.89 (s), 129.52 (s), 128.50 (d, J = 2.3 Hz), 127.92 (s), 125.29 (s), 123.13 (s), 121.44 (s), 121.01 (s), 120.51 (s), 118.20 (s), 117.77 (s), 117.41 (s), 113.23 (d, J = 7.5 Hz), 112.53 (s), 63.18 (s), 57.35 (d, J = 17.0 Hz), 55.02 (d, J = 19.2 Hz), 53.44 (s), 40.54 (s), 35.60 (s), 31.72 (s), 31.37 (s), 29.79 (d, J = 3.9 Hz), 29.01 (dd, J = 24.5, 8.8 Hz), 26.53 (s), 22.61 (d, J = 1.6 Hz), 14.13 (d, J = 7.5 Hz).

HR-MS (MALDI-TOF) m/z calcd. For ($C_{110}H_{121}ClN_{12}O_2S_4$): [M+H]:1805.831. Found:

1805.838.

2. Measurements and Characterizations

Molecular weights of the polymers were measured on Agilent Technologies PL-GPC 220 high-temperature-chromatograph at 150 °C using a calibration curve of polystyrene standards. Thermo gravimetric analysis (TGA) was recorded on Diamond TG/DTA under the protection of nitrogen at a heating rate of 10 °C /minute. UV-vis spectra were conducted with Lambda-950 (Perkin Elmer Instruments Co. Ltd., America). Cyclic voltammetry (CV) measurements were carried out using an electrochemical workstation equipped with a standard three-electrode configuration. Typically, a three-electrode cell equipped with Pt plate coated with a thin film as a working electrode, an Ag/AgCl (0.01 M in anhydrous acetonitrile) reference electrode, and a Pt wire counter electrode was employed. The measurements were done in anhydrous acetonitrile with tetrabutylammonium hexafluorophosphate (0.1 M) as the supporting electrolyte under an argon atmosphere at a scan rate of 100 mV/s. The potential of the Ag/AgCl reference electrode was internally calibrated by using the ferrocene/ferrocenium redox couple (Fc/Fc^+). The highest occupied molecular orbital (HOMO) and lowest unoccupied molecular orbital (LUMO) energy levels of polymers were calculated from the onset oxidation potential φ_{ox} and onset reductive potential φ_{red}, according to the formula of $E_{LUMO/HOMO} = -e(\varphi_{red/ox} + 4.8 - \varphi_{Fc/Fc^+})$ (eV).

The current density-voltage $J-V$ curves were measured in the glove box with a Keithley 2420 source measure unit. The photocurrent was obtained under illumination using an Oriel Newport 150W solar simulator (AM 1.5G), and the light intensity was

calibrated with a Newport reference detector (Oriel PN 91150 V). The EQE measurements of the devices were performed in air with an Oriel Newport system (Model 66902). Atomic force microscopy (AFM) images were obtained on a Multimode 8 in tapping mode.

The carrier mobilities of the polymer were investigated by the space charge limited current (SCLC) method. The hole mobility of the blend films was measured with the device structure of ITO/PEDOT: PSS/active layer /Au (80 nm), while the electron mobility of the blends was measured with the device structure of ITO/isopropanol liquid (TIPD) /active layer/Al (80 nm). The SCLC model is described by modified Mott-Gurney law:

$$J = \frac{9}{8}\varepsilon_0\varepsilon_r\mu\frac{V^2}{L^3}$$

Where J is the current density, ε_r is the dielectric constant of the active layer, ε_0 is the vacuum permittivity, μ is the mobility of the hole or electron, and L is the thickness of the active layer, V is the internal voltage in the device.

3. Photovoltaic Device Fabrication

The OSCs devices were fabricated with a conventional structure of ITO/PEDOT: PSS/active layer/ PFN-Br /Al. A thin layer of PEDOT: PSS was spin-casted on pre-cleaned ITO-coated glass at 3000 rpm. After baking at 150°C for 15 min, the substrates were transferred into the glove box. Optimized devices were prepared under the following conditions. The Donor: Acceptor (D: A) ratio of 1:1 (w/w) for **TTC-Cl: BTA3** and **TTC-Cl: HCl-BTA3** was dissolved chloroform (CF) with a total concentration of 15 mg/mL for 45 minutes at 60°C. The active layers were spin-coated

(3200 rpm) from the above solution with thermal annealing of 170℃ for 10 min. A PFN-Br layer was spin-coated on the top of all the active layers at 3000 rpm for 30 s. PFN-Br was dissolved in methanol at a concentration of 0.5 mg/mL. The Donor: Acceptor (D: A) ratio of 1:1 (w/w) for **TTC-Cl: HCl-BTA3** was dissolved chloroform (CF) with a total concentration of 15 mg/mL for 45 minutes at 60°C. The active layers were spin-coated (2500 rpm) from the above solution with thermal annealing of 170℃ for 10 min. A PFN-Br layer was spin-coated on the top of all the active layers at 3000 rpm for 30 s. PFN-Br was dissolved in methanol at a concentration of 0.5 mg/mL. The Donor: Acceptor (D: A) ratio of 1:1.2 (w/w) for **TTC-Cl: HCl-BTA3** was dissolved chloroform (CF) with a total concentration of 15 mg/mL for 45 minutes at 60°C. The active layers were spin-coated (3000 rpm) from the above solution with thermal annealing of 170℃ for 10min. A PFN-Br layer was spin-coated on the top of all the active layers at 3000 rpm for 30 s. Finally, an Al (80 nm) metal top electrode was thermal evaporated onto the active layer under about 4×10^{-4} Pa. The active area of the device was 0.04 cm^2 defined by the shadow mask.

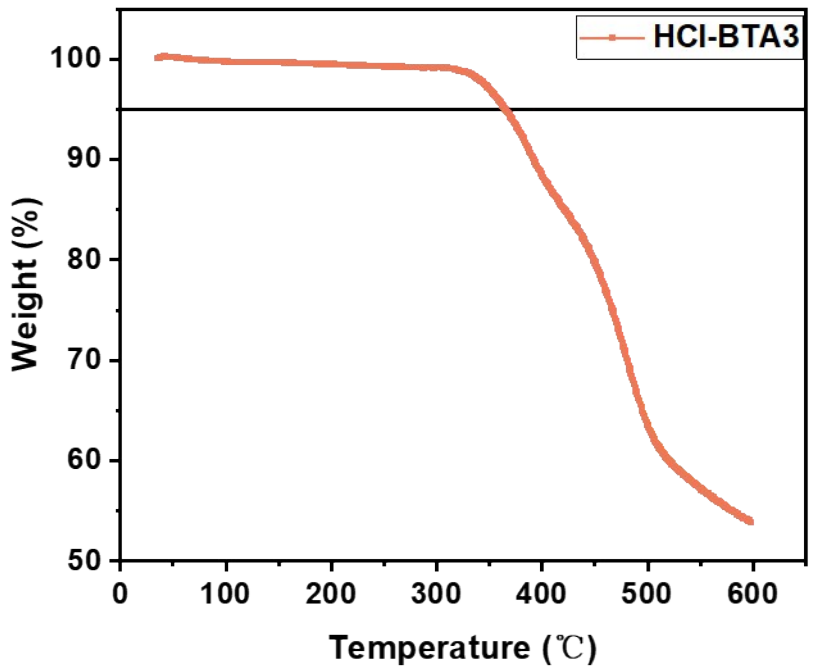

Figure S1. The thermal gravimetric analysis (TGA) curve of **HCl-BTA3**.

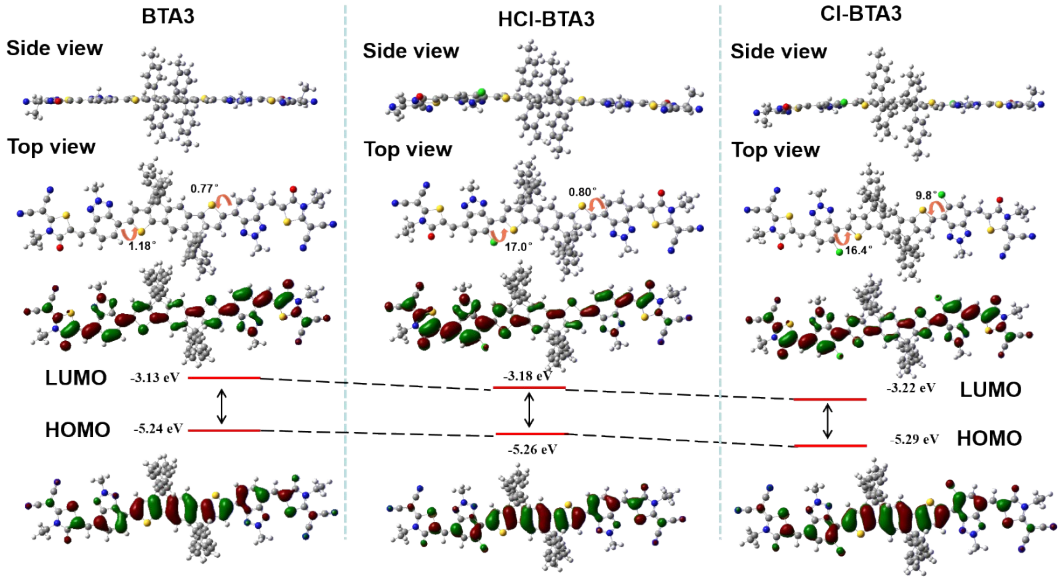

Figure S2. Optimized geometries and molecular orbitals of the BTA3, HCl-BTA3 and Cl-BTA3 calculated at the tuned B3LYP/6-31G(d) level. The side chains were replaced with methyl groups.

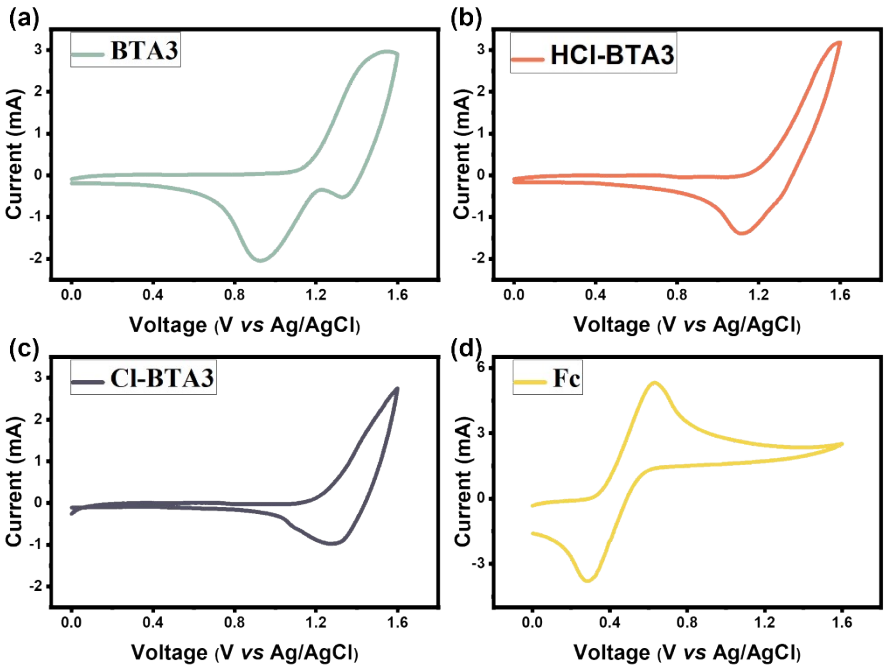

Figure S3. Cyclic voltammograms of (a) **BTA3,** (b**) HCl-BTA3**, (c) **Cl-BTA3** and (d) **Fc/Fc**$^{+}$, with Ag/AgCl as a reference electrode.

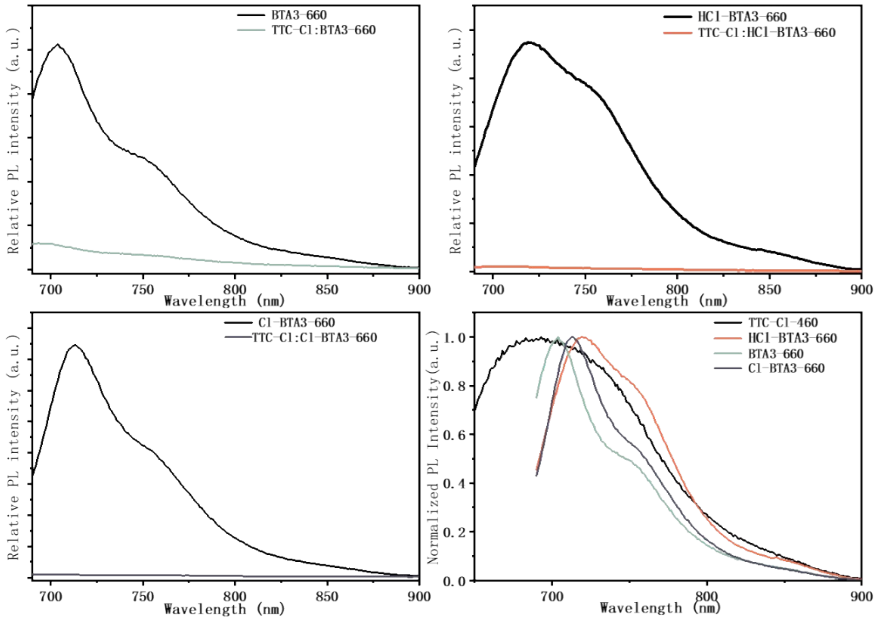

Figure S4. Photoluminescence spectra of the blend films under excitation at 660 nm, polymer donor neat films under excitation at 490 nm and the neat acceptor films under excitation at 660 nm;

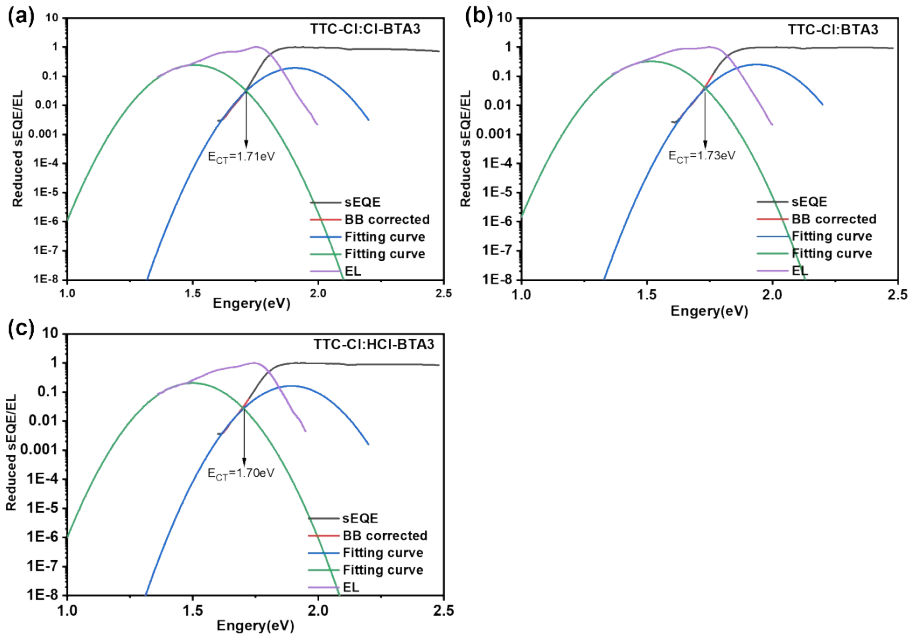

Figure S5. Reduced sEQE and EL spectra of the solar cells based on **TTC-Cl**: **BTA3** (a) and **TTC-Cl**: **HCl-BTA3** (b), and **TTC-Cl**: **Cl-BTA3** (c). The spectral line shape

of the low energy part of the sEQE spectrum is calculated from the electroluminescence spectrum using equation $\frac{EL(E)}{BB(E)}$. Fittings (red dashed curves) are done using the following equation for the sEQE spectrum to determine ECT: $EQE(E) = \frac{f}{E\sqrt{4\pi\lambda KT}exp}\left[\frac{-(E_{CT}+\lambda-E)^2}{4\lambda KT}\right]$ (color online).

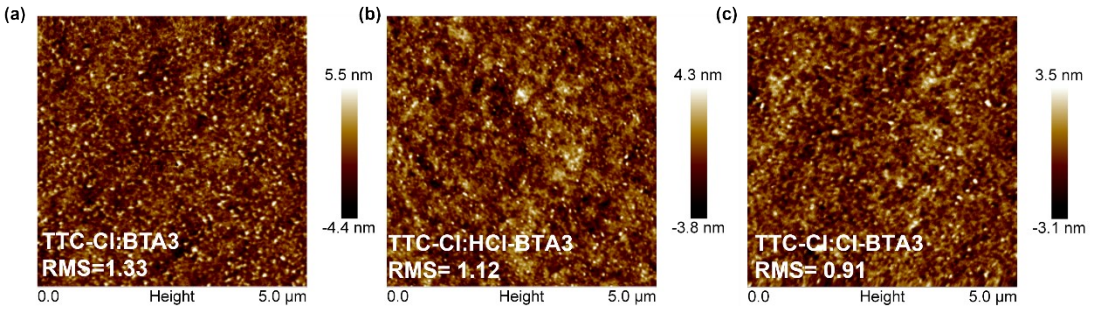

Figure S6. AFM height of (a) **TTC-Cl**: **BTA3**, (b) **TTC-Cl**: **HCl-BTA3** and (c) **TTC-Cl**: **Cl-BTA3** based blend films.

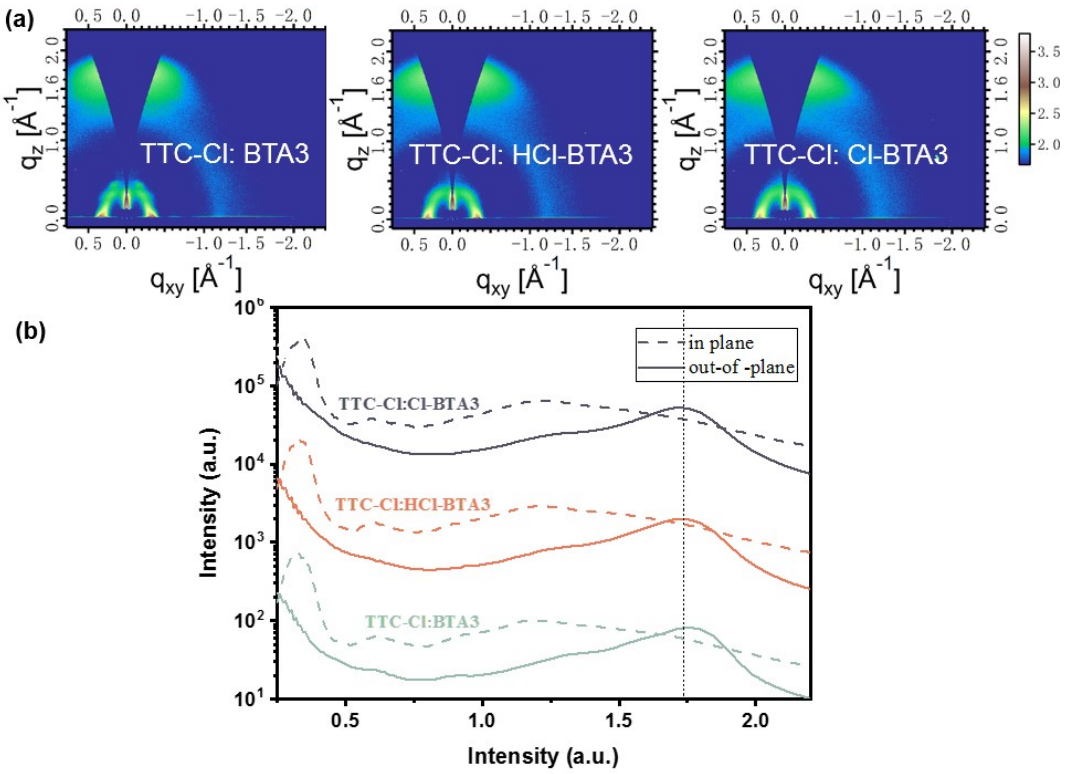

Figure S7. (a)2D-GIWAXS patterns of three blend films and (b) the related OOP and IP line cuts of the 2D GIWAXS patterns.

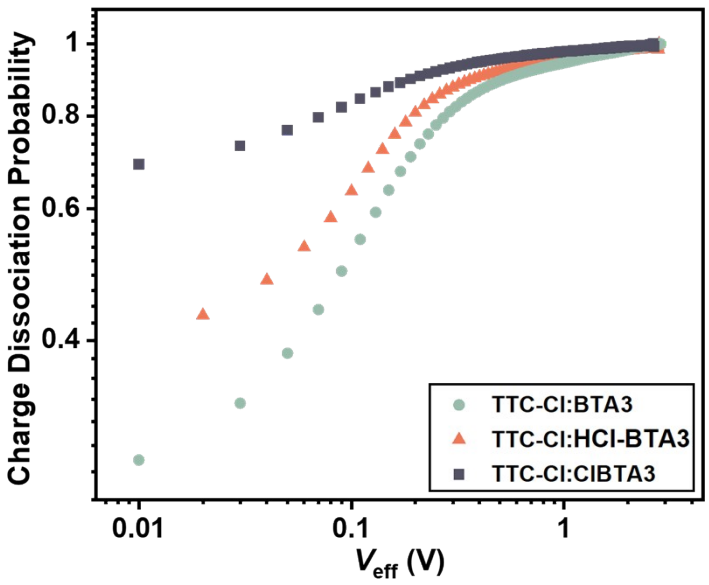

Figure S8. Plot of exciton dissociation probabilities (P_{diss}s) verse effective voltage (V_{eff}).

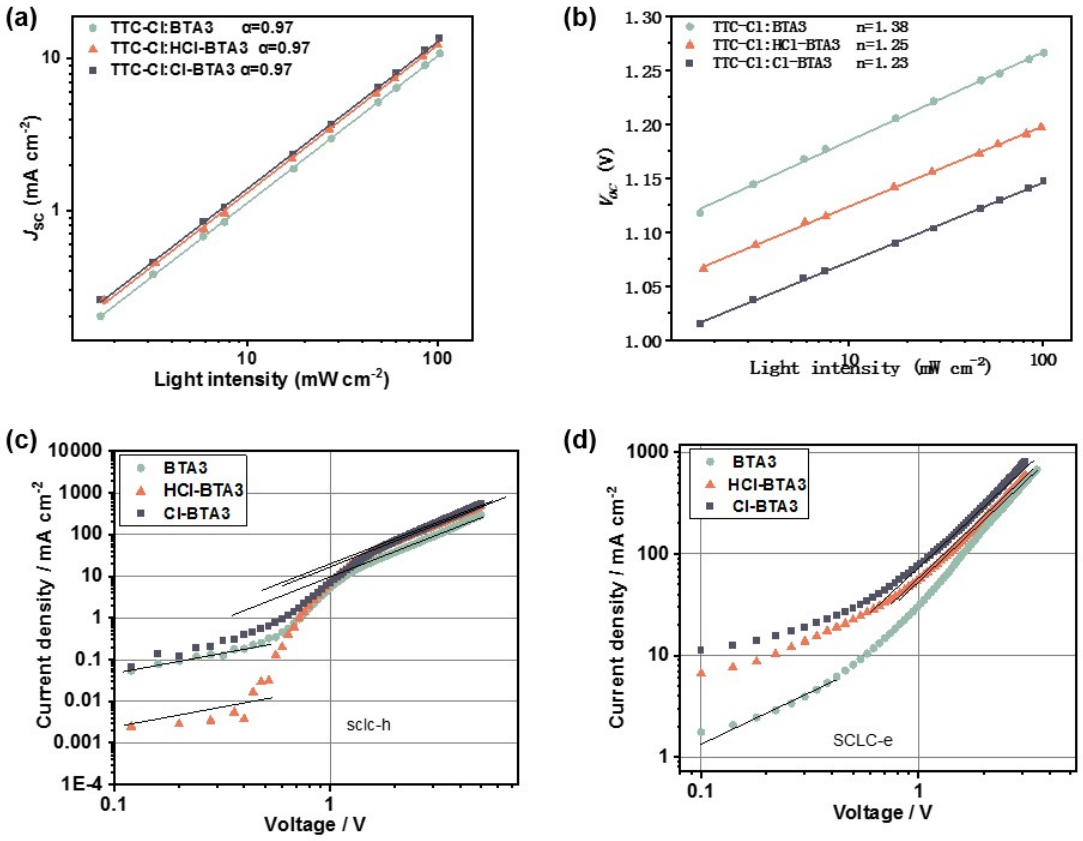

Figure S9 (a) Dependence of J_{SC} on light intensity; (b) Dependence of V_{OC} on light intensity; (c) hole mobility and (d) electron mobility of the optimized devices.

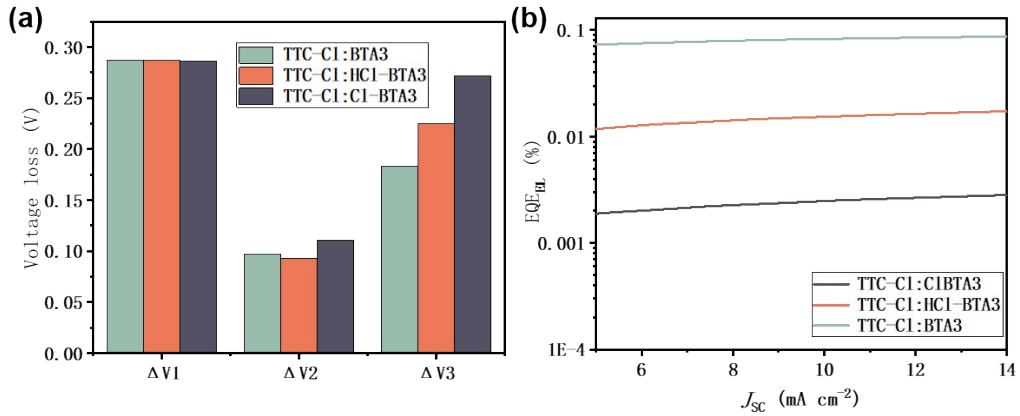

Figure S10. (a). Histogram of each part of the voltage losses in these four devices; (b) EL external quantum efficiencies (EQE_{EL}) of the four solar cells at various injected current densities.

Table S1. The optoelectrical properties of **BTA3**, **HCl-BTA3** and **Cl-BTA3**.

Compounds	λ_{max} [a] (nm)	λ_{max} [b] (nm)	λ_{onset} [c] (nm)	E_g^{opt} [d] (eV)	E_{HOMO} (eV)	E_{LUMO} (eV)
BTA3	-	654	713	1.74	-5.48	-3.74
HCl-BTA3	608	659	722	1.72	-5.50	-3.78
Cl-BTA3	-	662	720	1.72	-5.55	-3.83

[a] λ_{max} in CF solution at 25 °C. [b] λ_{max} in films. [c] Determined from the absorption onset of the thin film. [d] $E_g^{opt} = 1240/\lambda_{onset}$.

Table S2. The photovoltaic performance of devices under different weight ratios of donor/acceptor.

devices	D:A	V_{OC} (V)	J_{SC}(mA cm^{-2})	FF (%)	PCE(%)
TTC-Cl：BTA3	1.2:1	1.27	11.15	65.24	9.27 (9.14±0.07)
	1:1	1.26	11.30	67.89	9.67 (9.48±0.15)
	1:1.2	1.25	10.97	68.10	9.41 (9.24±0.15)
	1:1.5	1.26	10.59	65.97	8.85 (8.80±0.04)
TTC-Cl：HCl-BTA3	1.2:1	1.20	12.73	66.92	10.50 (10.45±0.07)
	1:1	1.2	13.19	69.56	11.20 (11.04±0.11)
	1:1.2	1.20	13.0	68.57	10.99 (10.85±0.11)
	1:1.5	1.20	12.74	67.37	10.37 (10.26±0.04)
TTC-Cl：Cl-BTA3	1.2:1	1.14	13.62	68.67	10.78 (10.62±0.09)
	1:1	1.15	13.37	70.68	10.87 (10.71±0.12)
	1:1.2	1.15	13.81	69.57	11.05 (10.96±0.09)
	1:1.5	1.15	13.03	69.58	10.48 (10.44±0.09)

Table S3. The photovoltaic performance of devices under different thermal annealing temperatures.

devices	Annealing temperature (°C)	V_{OC} (V)	J_{SC} (mA cm^{-2})	FF (%)	PCE (%)
TTC-Cl：BTA3	150	1.26	11.33	64.41	9.33 (9.19±0.14)
	170	1.26	11.30	67.89	9.67 (9.48±0.15)
	190	1..27	9.90	66.46	8.33 (8.17±0.10)
TTC-Cl：HCl-BTA3	130	1.22	12.17	60.08	9.07 (8.95±0.35)
	150	1.20	13.08	64.28	10.34 (10.14±0.09)
	170	1.20	13.19	69.56	11.20 (11.04±0.11)
	190	1.20	12.70	69.29	10.82 (10.70±0.03)
TTC-Cl：Cl-BTA3 (1:1)	150	1.16	12.42	70.87	10.25 (10.14±0.10)
	170	1.15	13.37	70.68	10.87 (10.71±0.12)
	190	1.15	13.05	70.51	10.56 (10.38±0.17)

Table S4. The photovoltaic performance of devices under different solvent additives.

devices	solvent additive	V_{OC} (V)	J_{SC} (mA cm^{-2})	FF (%)	PCE (%)
TTC-C: BTA3	NO	1.26	11.30	67.89	9.67 (9.48±0.15)
	0.25%DIO	1.27	10.75	67.08	9.26 (9.42±0.22)
	0.25%CN	1.26	10.55	65.43	8.82 (8.72±0.05)
	0.3%DPE	1.27	11.15	64.76	9.28 (9.27±0.04)
TTC-Cl：HCl-BTA3	NO	1.20	13.19	69.56	11.20 (11.04±0.11)
	0.25%DIO	1.20	13.12	67.26	10.66

					(10.53±0.05)
	0.5%DIO	1.21	12.24	66.42	9.84 (9.79±0.10)
	0.5%CN	1.20	7.17	61.36	5.32 (4.87±0.34)
	0.4%DPE	1.21	13.29	67.38	10.88 10.53±0.17
	0.8%DPE	1.20	13.50	66.27	10.82 (10.41±0.15)
TTC-Cl: Cl-BTA3	NO	1.15	13.81	69.57	11.05 (10.96±0.09)
	0.25%CN	1.15	13.13	69.20	10.58 (10.58±0.10)
	0.25%DIO	1.15	13.18	69.61	10.67 (10.67±0.02)
	0.3%DPE	1.14	13.16	67.21	10.25 (10.15±0.08)

Table S5. The detailed voltage loss and energetic disorder data of the three devices.

Devices	E_g **(eV)**	V_{oc} **(V)**	V_{oc}^{SQ} **(V)**	E_g/q-V_{oc}^{SQ} **(V)**	V_{oc}^{rad} **(V)**	V_{oc}^{SQ}-V_{oc}^{rad} **(V)**	EQE_{EL} **(%)**	$\Delta V_{oc}^{non\text{-}rad}$ **(V)**	E_u **(meV)**
TTC-Cl : BTA3	1.826	1.260	1.539	0.287	1.443	0.097	8.49×10^{-2}	0.183	38.95
TTC-Cl : HCl-BTA3	1.807	1.201	1.519	0.287	1.427	0.093	1.66×10^{-2}	0.225	37.11
TTC-Cl : Cl-BTA3	1.806	1.152	1.519	0.286	1.424	0.095	2.77×10^{-3}	0.272	37.08

1. B. Xiao, A. Tang, J. Zhang, A. Mahmood, Z. Wei and E. Zhou, *Adv. Energy Mater.*, 2017, **7**, 1602229.
2. T. Dai, Q. Nie, P. Lei, B. Zhang, J. Zhou, A. Tang, H. Wang, Q. Zeng and E. Zhou, *ACS Appl. Mater. Interfaces*, 2021, **13**, 58994-59005.